A combined thermodynamics and first principles study of the electronic, lattice and magnetic contributions to the magnetocaloric effect in $La_{0.75}Ca_{0.25}MnO_3$

R. K. Korotana[1] G. Mallia[1], N. M. Fortunato[2],

J. S. Amaral[2,3], Z. Gercsi[4], and N. M. Harrison[1*]

[1] *Thomas Young Centre, Department of Chemistry,*

Imperial College London, South Kensington, London SW7 2AZ, UK

[2] *Departamento de Física and CICECO,*

Universidade de Aveiro, 3810-193 Aveiro, Portugal

[3] *IFIMUP and IN-Institute of Nanoscience and Nanotechnology, 4169-007 Porto, Portugal*

[4] *CRANN and School of Physics, Trinity College Dublin - Dublin 2, Ireland*

(Dated: February 13, 2016)

Abstract

Manganites with the formula $La_{1-x}Ca_xMnO_3$ for $0.2 < x < 0.5$ undergo a magnetic field driven transition from a paramagnetic to ferromagnetic state, which is accompanied by changes in the lattice and electronic structure. An isotropic expansion of the $La_{0.75}Ca_{0.25}MnO_3$ cell at the phase transition has been observed experimentally. It is therefore expected that there will be a large entropy change at the transition due to the first order nature. However, the maximum obtained value for the entropy change in Ca-doped manganites merely reaches a moderate value in the field of a permanent magnet. The present theoretical work aims to shed light on this discrepancy. A combination of finite temperature statistical mechanics and first principles theory is applied to determine individual contributions to the total entropy change of the system by treating the electronic, lattice and magnetic components independently. Hybrid-exchange density functional (B3LYP) calculations and Monte Carlo simulations are performed for $La_{0.75}Ca_{0.25}MnO_3$. Through the analysis of individual entropy contributions, it is identified that the electronic and lattice entropy changes oppose the magnetic entropy change. The results highlighted in the present work demonstrate how the electronic and vibrational terms can have a deleterious effect on the total entropy change.

* romi.korotana09@alumni.imperial.ac.uk

I. INTRODUCTION

The Magnetocaloric Effect (MCE) [1–5] is defined as the change in temperature of a magnetically ordered material, upon the application or removal of an external magnetic field under adiabatic conditions. The effect was first discovered, in iron, by Emil Warburg in 1881 [6]. In the past two decades, there has been a surge of interest in magnetocaloric materials that could potentially be used in cooling devices, such as heat pumps and magnetic refrigerators [7–9]. More recently, manganites, an economically viable class of materials, have attracted much attention due to their remarkable structural and electronic properties, which are strongly dependent on the doping concentration as well as external variables, such as temperature, pressure, and electric or magnetic fields [4].

Manganites are perovskites, which have the general formula $R_{1-x}A_xMnO_3$, where R is a trivalent rare earth metal and A is a divalent alkaline earth element. Such perovskites exhibit cross-coupling between the spin, charge, orbital and lattice degrees of freedoms [10–12]. This strong interplay often lead to non-trivial material responses to external stimuli. However, due to the effects of strong electron correlation, a complete microscopic understanding of the physics underlying the properties of manganites has not yet been obtained.

Since the discovery of the Collosal Magnetoresistance (CMR) [13–15], experimental studies on manganites doped with divalent alkaline earth elements, such as Ca, Ba and Sr, have been the subject of intense study. An important practical feature of manganites is that the average radii of cations at different sites can affect the ground state [2]. The structure of manganites, in particular, is very robust against chemical modifications at the A-site. Furthermore, doping at the R-site is of interest since the exchange interaction could be modified. This provides a mechanism for tuning the MCE and the Curie temperature T_C, where the latter defines the operating temperature of the cooling device.

The $La_{1-x}Ca_xMnO_3$ series undergoes a field driven transition from a paramagnetic insulating (PM-I) to ferromagnetic metallic (FM-M) state for $0.2 < x < 0.5$, which is accompanied by changes in the lattice and electronic structure. As determined by Radaelli *et.al.*, from high-resolution synchrotron X-ray powder diffraction data, an isotropic expansion of the $La_{0.75}Ca_{0.25}MnO_3$ cell occurs at the transition without affecting the orthorhombic symmetry [16]. It is therefore expected that the isothermal entropy change ΔS_{iso} for this particular composition would be considerable, since the electronic and lattice contributions

may play a significant role in enhancing the MCE in addition to the expected contribution from spin disorder [16, 17]. Despite many experimental efforts to enhance the ΔS_{iso} in $La_{1-x}Ca_xMnO_3$ manganites, particularly for $0.2 < x < 0.5$, the MCE reaches a modest value in the field of a permanent magnet [4, 14, 18–27]. For example, the maximum obtained value for $La_{0.75}Ca_{0.25}MnO_3$ is $4.70 Jkg^{-1}K^{-1}$ [24] for an applied external magnetic field of 1.5T.

The Gibbs free energy is expressed as [28]:

$$G(T, P, H) = U_{vib} + U_{elas} + U_{elec} + U_{ex} - MH + PV - TS \quad (1)$$

where the first four terms correspond to the internal energy (vibrational, elastic, electronic and magnetic, respectively). In the current study we make the fundamental assumption that the entropy change can be expressed as,

$$\Delta S_{total} = \Delta S_{vib} + \Delta S_{elas} + \Delta S_{elec} + \Delta S_{mag} \quad (2)$$

where ΔS_{vib}, ΔS_{elas}, ΔS_{elec} and ΔS_{mag} are the vibrational, elastic, electronic and magnetic contributions, respectively. Equ. 2 corresponds to the isothermal entropy change ΔS_{iso} when a magnetic field is applied, which can also be determined through integration of the thermodynamic Maxwell relation. This assumption neglects the explicit interactions between lattice, spin and electronic degrees of freedom. We test the assumption of independent contributions for a simple model with long translational order.

The paper is organized as follows: in Section II the computational methodology is provided and the results are presented in Section III. The discussion begins with the electronic entropy calculation for $La_{0.75}Ca_{0.25}MnO_3$, followed by an analysis of the lattice component, which includes both the elastic and vibrational contributions. The discussion then focuses on a Monte Carlo study of the magnetic entropy and magnetization dynamics of the doped manganite composition. Conclusions are drawn in Section IV.

II. METHODOLOGY

All calculations have been performed using CRYSTAL09 [29] which is based on the expansion of the crystalline orbitals as a linear combination of a local basis set (BS) consisting of atom centered Gaussian orbitals.

The Mn, O and Ca ions are described by a triple valence all-electron BS: an 86-411d(41) contraction (one s, four sp, and two d shells), an 8-411d(1) contraction (one s, three sp, and one d shells) and an 8-65111(21) contraction (one s, three sp, and two d shells), respectively; the most diffuse $sp(d)$ exponents are α^{Mn}=0.4986(0.249), α^{O}= 0.1843(0.6) and α^{Ca}= 0.295(0.2891) Bohr^{-2}. The La basis set includes a relativistic pseudopotential to describe the core electrons, while the valence part consists of a 411p(411)d(311) contraction scheme (with three s, three p and three d shells); the most diffuse exponent is α^{La}=0.15 Bohr^{-2} for each s, p and d [30].

Electron exchange and correlation are approximated using the B3LYP hybrid exchange functional, which is expected to be more reliable than LDA or GGA approaches for transition metal oxides [31–34]. The exchange and correlation potentials and energy functional are integrated numerically on an atom centered grid of points. The integration over radial and angular coordinates is performed using Gauss-Legendre and Lebedev schemes, respectively. A pruned grid consisting of 99 radial points and 5 sub-intervals with (146, 302, 590, 1454, 590) angular points has been used for all calculations (the XXLGRID option implemented in CRYSTAL09 [29]). This grid converges the integrated charge density to an accuracy of about $\times 10^{-6}$ electrons per unit cell. The Coulomb and exchange series are summed directly and truncated using overlap criteria with thresholds of 10^{-7}, 10^{-7}, 10^{-7}, 10^{-7} and 10^{-14} as described previously [29, 35]. Reciprocal space sampling was performed on a Pack-Monkhorst net with a shrinking factor IS=8, which defines 75 symmetry unique k-points in the Brillouin zone of the primitive cell. The self consistent field procedure was converged to a tolerance in the total energy of $\Delta E = 1 \cdot 10^{-7} E_h$ per unit cell.

The cell parameters and the internal coordinates have been determined by minimization of the total energy within an iterative procedure based on the total energy gradient calculated analytically with respect to the cell parameters and nuclear coordinates. Convergence was determined from the root-mean-square (rms) and the absolute value of the largest component of the forces. The thresholds for the maximum and the rms forces (the maximum and the rms atomic displacements) have been set to 0.00045 and 0.00030 (0.00180 and 0.0012) in atomic units. Geometry optimization was terminated when all four conditions were satisfied simultaneously.

The FM-PM phase transition has been investigated by mapping the first principles energies to the 3D Ising model in a Monte Carlo approach. A simple cubic lattice with periodic

boundary conditions is considered and it is assumed that interactions occur only between nearest neighbouring spin states. The Ising Hamiltonian, $\hat{H}^{mag}$ is defined as:

$$\hat{H}^{mag} = -\frac{1}{2}\sum_{\langle i,j\rangle} J_{ij} {S_i}^z {S_j}^z - \sum_i H_{ext} {S_i}^z \tag{3}$$

where H_{ext} is an external magnetic field, J_{ij} is the exchange parameter and S is the spin state, which can only take on the value -1 (spin *down*) or 1 (spin *up*). In the Ising model, only the z component of the spin variable is considered.

Here the relevant thermodynamic parameters such as the magnetization dependence on temperature and applied magnetic field, and corresponding MCE near $T_{\rm C}$ are numerically estimated via the random path sampling (RPS) Monte Carlo method [36]. The RPS method allows a flat magnetization sampling histogram of magnetic configurations, by construction. Energy and magnetization sampling is performed via local updates from +1 and -1 total magnetization states. Prior to each sweep, a shuffled list of spin positions is generated. Spin flips, where a spin in the +1 state is flipped with the probability of 1, are then performed sequentially using this list. The configuration energy is determined via the local energy difference due to a spin flip, as usually done in the Metropolis algorithm. From the obtained joint density of states (JDos), the partition function is evaluated for each desired (H, T) value and therefore, the corresponding thermodynamic variables and their (H, T) dependence. This approach compares favourably to the use of the Metropolis algorithm in the context of MCE studies, as critical slowing down effects near $T_{\rm C}$ are avoided, and individual (H, T)-dependent calculations are unnecessary, as the more time-consuming JDos evaluation is independent of these extensive parameters.

III. RESULTS

A. Electronic entropy

The metal-insulator (M-I) transition results in a modification of the density of states at the Fermi level, and strong evidence for this has been provided in a recent theoretical study of $La_{0.75}Ca_{0.25}MnO_3$ [37]. Thus, the electronic entropy for the M and I phases is expected to differ significantly. The electronic structure determined for the M and I, from hybrid density functional theory calculations [37], is used to compute the ΔS_{elec} for $La_{0.75}Ca_{0.25}MnO_3$. This

contribution is computed using the finite temperature DFT approach [38], which allows one to express the free energy in terms of the Fermi function,

$$f_{ik} = (1 + e^{\frac{(\epsilon_{ik} - \epsilon_F)}{k_b T}})^{-1}, \tag{4}$$

$$S_{electronic} = 2 \sum_{i,k}^{N_{states}} (f_{ik} ln f_{ik} + (1 - f_{ik}) ln(1 - f_{ik})) k_{i,weight}, \tag{5}$$

where N is the number of (occupied and unoccupied) states, f_{ik} is the Fermi distribution function and $k_{i,weight}$ is the k_i point geometrical weight, respectively. The Fermi function describes the probability of occupation at a certain temperature, which can be summed over all the k-points in the Brillouin zone for each band to determine the occupation levels.

Temperature (K)	ΔS_{elec} (Jmol^{-1}K^{-1})
10	0.01
100	0.19
224	0.45

TABLE I. The electronic entropy contribution ΔS_{elec} to ΔS for the FM-M (LCMO at x=1/4) at 10K, 100K and 224K (T_C=224K [20]), where S_{elec} for the FM-I is considered to be zero.

The computed values of the electronic entropy, ΔS_{elec} at 10K, 100K and 224K (T_C) are given in Table I. The values are positive, since S_{elec} for the insulator is zero and the field-driven transition is from an I to a M. Thus, as the temperature is increased from 10K to 224K, the ΔS_{elec} increases.

B. Lattice entropy

1. *Elastic contribution*

The elastic contribution to the total entropy change has been calculated from the following [28]:

$$\Delta S_{elas} = \frac{1}{T_C} \frac{B}{2} \left(\frac{\Delta V}{V} \right)^2 \tag{6}$$

where the value for the bulk elastic modulus B is taken to be 100GPa, which has been determined from the ultrasonic properties of $La_{0.67}Ca_{0.33}MnO_3$ [39]. The ΔV in this particular calculation corresponds to the difference in volume between the FM-M (244.8Å^3) and FM-I (245.1Å^3) state from the DFT calculations, which is 0.3Å^3 [37]. If the experimental T_C of 224K [18] is assumed, the ΔS_{elas} is 1.81×10^{-4}Jmol^{-1}K^{-1}. The elastic contribution to ΔS is therefore considered to be a negligible term. If, however, we assume the $\Delta V/V \approx 0.13\%$ determined from high-resolution synchrotron x-ray powder diffraction data [16], then the ΔS_{elas} is 2.03×10^{-4}Jmol^{-1}K^{-1}. Thus, the theoretical ΔS_{elas} value is also negligibly small.

2. Vibrational contribution

In order to sample all the vibrational modes, the vibrational frequencies for an isotropic (80 atom) supercell computed to determine the vibrational contribution S_{vib} to ΔS in the simple harmonic approximation. The mass-weighted Hessian (or dynamical) matrix [40] is calculated by numerical evaluation of the first derivative of the analytical atomic gradients; ~~the eigenvalues of the Hessian matrix correspond to the vibrational frequencies.~~ The vibrational entropy S_{vib} has been calculated using the following,

$$F_{vib} = E_0 + \frac{1}{2}\sum_{k,j}\hbar\omega + k_B T \sum_{k,j} ln\left[1 - exp(-\hbar\omega/k_B T)\right] \tag{7}$$

$$S_{vib} = -\frac{\partial F_{vib}}{\partial T} \tag{8}$$

The S_{vib} for the metallic and insulating state is given in Table II.

M/I	S_{vib} (Jmol^{-1}K^{-1})
M	92.97
I	88.33
ΔS_{elec}	*4.64*

TABLE II. The vibrational entropy for LCMO at x=1/4, in the FM-M and FM-I states for the supercell. The ΔS_{vib} is given in italics in units of Jmol^{-1}K^{-1}.

The S_{vib} for the metal is higher than that of the insulator, as expected. This is attributed

to phonon mode softening in the metallic state. Therefore, the contribution of ΔS_{vib} is also positive.

C. Magnetic entropy

The Ising Hamiltonian has been parameterised with the exchange coupling constant of 6.69meV calculated by averaging the apical (J_{ap}) and equatorial (J_{eq}) determined from hybrid-exchange DFT calculations for the FM-M state [37]. The $Mn^{3.75+}$ is described by a classical Ising spin, and the La, Ca and O ions are considered to be non-magnetic in the MC simulations. The number of sites used in the simulation of a simple cubic (SC) lattice is 64, and the magnetization values were obtained by finding the minumum of the free energy evaluated from the partition function at the desired (H, T) values. The number of RPS sweeps performed was 10^{11}, leading to a free energy convergence better than 0.001% for T near T_C, under zero applied field. The magnetic entropy has then been computed as:

$$\Delta S_{mag}(T, \Delta H) = \int_{H_0}^{H_1} \left(\frac{\partial M(T,H)}{\partial T} \right)_H \mathrm{d}H. \tag{9}$$

The field-induced magnetic entropy change ΔS_{mag} has been computed for ΔH of 1 and 2T and is shown in Fig. 1.

The predicted $T_C \sim 398$K has been determined from the peak in the ΔS_{mag} curve. The calculated T_C, for the bulk crystal, is somewhat larger than the T_C values of 177K and 224K determined from magnetization measurements (defined as the maximum slope in dM/dT) of $La_{0.75}Ca_{0.25}MnO_3$ nanoparticles which varied in size [20]. The maxima of the field-induced ΔS_{mag} occurs in the vicinity of T_C and the determined values for ΔH of 1 and 2 T are -0.284 and -0.438 $Jmol^{-1}K^{-1}$, respectively. The computed values are significantly smaller than the experimental ΔS_{iso} calculated from magnetization measurements of $La_{0.75}Ca_{0.25}MnO_3$ for an applied magnetic field of 1.5T [18].

IV. CONCLUSIONS

A combined hybrid-exchange DFT and Monte Carlo approach has been used to quantify the electronic, lattice and magnetic entropy contributions, to the entropy change ΔS across

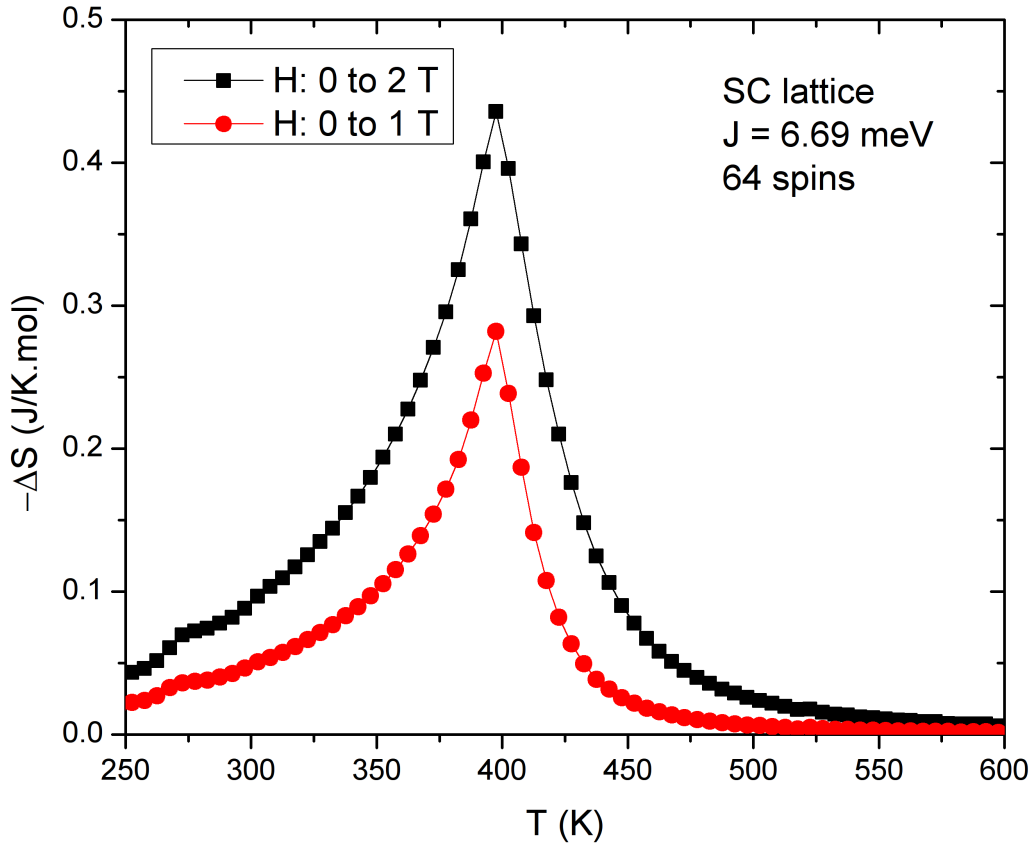

FIG. 1. The magnetic entropy change ΔS_{mag} due to an applied magnetic field of 1 and 2T as a function of temperature calculated for J=6.69meV.

the PM-I to FM-M transition, in $La_{0.75}Ca_{0.25}MnO_3$. It has been predicted that the electronic and magnetic contributions are of a similar magnitude. Further, the computed electronic and lattice entropy terms oppose the magnetic one. Thus, the electronic and vibrational terms have a destructive effect on the total entropy change. The formalism adopted herein has provided a valuable insight into the competing entropy components for $La_{0.75}Ca_{0.25}MnO_3$. The effects of more complex interactions such as spin-lattice and spin-orbit on the entropy change should be considered. However, MC simulations of a magnetovolume coupled Ising hamiltonian would require J values dependent on lattice volume which is computationally expensive. The microscopic optimization of such interactions, to enhance the magnetocaloric properties, may become a valuable tool in the search for new magnetocaloric materials.

ACKNOWLEDGMENTS

We thank L. F. Cohen, K. G. Sandeman and J. A. Turcaud of The Blackett Laboratory, Imperial College London for useful discussions. This work was developed within the scope of the project CICECO-Aveiro Institute of Materials, POCI-01-0145-FEDER-007679 (FCT Ref. UID/CTM/50011/2013), financed by national funds through the FCT/MEC and when appropriate co-financed by FEDER under the PT2020 Partnership Agreement. JSA acknowledges FCT SFRH/BPD/63942/2009 grant. The EPSRC Grant (EP/G060940/1) on Nanostructured Functional Materials for Energy Efficient Refrigeration, Energy Harvesting and Production of Hydrogen from Water is gratefully acknowledged. This work made use of the high performance computing facilities of Imperial College London andvia membership of the UKs HPC Materials Chemistry Consortium funded by EPSRC (EP/F067496)of HECToR, the UKs national high-performance computing service, which is provided by UoE HPCx Ltd. at the University of Edinburgh, Cray Inc. and NAG Ltd., and funded by the Office of Science and Technology through EPSRC.

---

[1] J. R. Gómez, R. F. Garcia, A. D. M. Catoira, and M. R. Gómez, Renew. Sust. Energ. Rev. **17**, 74 (2013).

[2] V. Franco, J. Blázquez, B. Ingale, and A. Conde, Annu. Rev. Mater. Res. **42**, 305 (2012).

[3] K. G. Sandeman, Scripta Mater. **67**, 566 (2012).

[4] M. Phan and S. Yu, J. Magn. Magn. Mater. **308**, 325) (2007).

[5] Int. J. Refrig. **29**, 1239 (2006).

[6] E. Warburg, Ann. Phys. **13**, 141 (1881).

[7] B. F. Yu, M. Liu, and P. W. Egolf, Int. J. Refrig. **33**, 10291060 (2010).

[8] A. Rowe, Int. J. Refrig. **34**, 168 (2011).

[9] K. K. Neilsen, J. Tusek, K. Engelbrecht, S. Schopfer, and A. Schopfer, Int. J. Refrig. **34**, 603 (2011).

[10] C. N. R. Rao and B. Raveau, *Collosal Magnetoresistance, Charge Ordering and Related Properties of Managese Oxides* (World Scientific, Singapore, 1998).

[11] E. Dagotto, T. Hotta, and A. Moreo, Phys. Rep. **344**, 1 (2001).

[12] Y. Tokura, *Collosal Magnetoresistance Oxides* (Gordon and Breach, London, 1999).

[13] G. H. Jonker and J. H. Santen, Physica **16**, 337 (1950).

[14] A. J. Morelli, A. M. Mance, J. V. Mantese, and A. L. Micheli, J. Appl. Phys **79**, 373 (1996).

[15] M. B. Salamon and M. Jaime, Rev. Mod. Phys. **73**, 583 (2001).

[16] P. G. Radaelli, D. E. Cox, M. Marezio, S.-W. Cheong, P. E. Schiffer, and A. P. Ramirez, Phys. Rev. Lett. **75**, 4488 (1995).

[17] K. H. Kim, J. Y. Gu, H. S. Choi, G. W. Park, and T. W. Noh, Phys. Rev. Lett. **77**, 1877 (1996).

[18] Z. B. Guo, J. R. Zhang, H. Huang, W. P. Ding, and Y. W. Du, Appl. Phys. Lett. **70**, 904 (1997).

[19] M. H. Phan, V. T. Pham, S. Yu, and J. R. Rhee, J. Magn. Magn. Mater. **272-276**, 2337 (2004).

[20] H. H. W. P. D. Y. W. D. Z. B. Guo, J. R. Zhang, Appl. Phys. Lett. **70**, 904 (1996).

[21] M. H. Phan, S. Yu, N. H. Hur, and Y. H. Yeong, J. Appl. Phys. **96**, 1154 (2004).

[22] M. H. Phan, S. B. Tian, S. Yu, and N. H. Hur, Physica B **327**, 211 (2003).

[23] Q. Y. Xu, K. M. Gu, X. L. Liang, G. Ni, Z. M. Wang, H. Sang, and Y. W. Du, J. Appl. Phys. **90**, 524 (2001).

[24] X. X. Zhang, J. Tejada, Y. Xin, G. F. Sun, K. W. Wong, and X. Bohigas, Appl. Phys. Lett. **69**, 3596 (1996).

[25] L. E. Hueso, P. Sande, D. R. Miguens, J. Rivas, F. Rivadulla, and M. A. Lopez-Quintela, J. Appl. Phys. **91**, 9943 (2002).

[26] Y. Sun, X. Xu, and Y. H. Zhang, J. Magn. Magn. Mater. **219**, 183 (2000).

[27] X. Bohigas, J. Tejada, M. L. Marinez-Sarrion, S. Tripp, and R. Black, J. Magn. Magn. Mater. **208**, 85 (2000).

[28] L. Jia, G. J. Liu, J. R. Sun, H. W. Zhang, F. X. Hu, C. Dong, G. H. Rao, and B. G. Shen, J. App. Phys. **100**, 1239041 (2006).

[29] R. Dovesi, V. R. Saunders, C. Roetti, R. Orlando, C. M. Zicovich-Wilson, F. Pascale, B. Civalleri, K. Doll, N. M. Harrison, I. J. Bush, P. Dco, and M. Llunell, *CRYSTAL09 User's Manual* (University of Torino, Torino, 2009).

[30] D. M. noz, N. M. Harrison, and F. Illas, Phys. Rev. B **69**, 085115 (2004).

[31] J. Muscat and N. M. Harrison, Chem. Phys. Lett. **342**, 2016 (2001).

[32] F. Cora, M. Alfredsson, G. Mallia, D. S. Middlemiss, W. C. Mackrodt, R. Dovesi, and R. Orlando, *The Performance of Hybrid Density Functionals in Solid State Chemistry*, Vol. 113 (Springer, Berlin, 2004).

[33] C. Adamo, M. Ernzerhof, and G. E. Scuseria, J. Chem. Phys. **112**, 2643 (2000).

[34] S. Kurth, J. P. Perdew, and P. Blaha, Int. J. Quantum Chem. **75**, 889 (1999).

[35] C. Pisani, R. Dovesi, and C. Roetti, *Hartree-Fock ab initio Treatment of Crystalline Systems, vol. 48 of Lecture Notes in Chemistry* (Springer Verlag, Heidelberg, 1988).

[36] J. S. Amaral, J. N. Goncalves, and V. S. Amaral, IEEE Trans. Magn. **50**, 1 (2014).

[37] R. Korotana, G. Mallia, Z. Gercsi, L. Liborio, and N. M. Harrison, Phys. Rev. B **89**, 205110 (2014).

[38] N. D. Mermin, Phys. Rev. **137**, 1441 (1965).

[39] C. Zhu, R. Zheng, J. Su, and J. He, Appl. Phys. Lett. **74**, 3504 (1999).

[40] F. Pascale, C. M. Zicovich-Wilson, F. L. Gejo, B. Civalleri, R. Orlando, and R. Dovesi, J. Comput. Chem. **25**, 888 (2004).